Beware of fake ν's: The effect of massive neutrinos on the nonlinear evolution of cosmic structure

Adrian E. Bayer,[1,2,*] Arka Banerjee,[3,4,†] and Uroš Seljak[1,2,5,‡]

[1]*Berkeley Center for Cosmological Physics, University of California, Berkeley, California 94720, USA*
[2]*Department of Physics, University of California, Berkeley, California 94720, USA*
[3]*Department of Physics, Indian Institute of Science Education and Research, Homi Bhabha Road, Pashan, Pune 411008, India*
[4]*Fermi National Accelerator Laboratory, Cosmic Physics Center, Batavia, Illinois 60510, USA*
[5]*Lawrence Berkeley National Laboratory, Physics Division, 1 Cyclotron Road, Berkeley, California 94720, USA*

(Received 13 August 2021; accepted 6 May 2022; published 14 June 2022)

Massive neutrinos suppress the growth of cosmic structure on small, nonlinear scales. It is thus often proposed that using statistics beyond the power spectrum can tighten constraints on the neutrino mass by extracting additional information from these nonlinear scales. We study the information content regarding neutrino mass at the field level, quantifying how much of this information arises from the difference in nonlinear evolution between a cosmology with one fluid [cold dark matter (CDM)] and two fluids (CDM + neutrinos). We do so by running two N-body simulations, one with and one without massive neutrinos, both with the same phases, and matching their linear power spectrum at a given low redshift. This effectively isolates the information encoded in the linear initial conditions from the nonlinear cosmic evolution. We demonstrate that, for $k \lesssim 1\ h/\mathrm{Mpc}$, and for a single redshift, there is negligible difference in the real-space CDM field between the two simulations. This suggests that all the information regarding neutrino mass is in the linear power spectrum set by the initial conditions. Thus, any probe based on the CDM field alone will have negligible constraining power beyond that which exists at the linear level over the same range of scales. Consequently, any probe based on the halo field will contain little information beyond the linear power. We find similar results for the matter field responsible for weak lensing. We also demonstrate that there may be much information beyond the power spectrum in the 3D matter field; however, this is not observable in modern surveys via dark matter halos or weak lensing. Finally, we show that there is additional information to be found in redshift space.

DOI: 10.1103/PhysRevD.105.123510

I. INTRODUCTION

Upcoming cosmological missions, such as those by the Dark Energy Spectroscopic Instrument [1], Euclid [2], Legacy Survey of Space and Time (LSST) [3], Prime Focus Spectrograph [4], Square Kilometre Array [5], and Wide Field Infrared Survey Telescope [6], will probe progressively smaller scales of cosmic structure. It is hoped that by probing these small, nonlinear scales one will be able to detect much information regarding the total neutrino mass. To fully realize the potential of these surveys, an urgent task is thus to quantify and optimally extract this information from the observed cosmological fields.

In a cosmology with massive neutrinos [7], we can define ρ_{cb} as the contribution to the energy density due to cold dark matter (CDM) and baryons, ρ_ν as the contribution due to neutrinos, and ρ_m as the total matter contribution. Given the lower bound on the sum of the neutrino masses coming from oscillation experiments is $M_\nu = 60$ meV [8–12], neutrinos are nonrelativistic at low redshift. Defining $\bar{\rho}_X$ as the mean energy density in species X, where $X = \{cb, \nu, m\}$, we can further define the relative overdensity of species X at redshift 0 as $\delta_X = (\rho_X - \bar{\rho}_X)/\bar{\rho}_X$ and the fraction of the total matter density in species X as $f_X = \bar{\rho}_X/\bar{\rho}_m = \Omega_X/\Omega_m$. This gives

$$\Omega_m \delta_m = \Omega_{cb}\delta_{cb} + \Omega_\nu \delta_\nu \tag{1}$$

and the matter overdensity as

$$\delta_m = (1 - f_\nu)\delta_{cb} + f_\nu \delta_\nu. \tag{2}$$

In practice, we cannot measure δ_ν directly, as we do not have direct access to fluctuations in the cosmic neutrino background. We also cannot measure $f_\nu = \Omega_\nu/\Omega_m$ directly

*abayer@berkeley.edu
†arka@iiserpune.ac.in
‡useljak@berkeley.edu

at low redshifts from the redshift-distance relations, since neutrinos are nonrelativistic and their density has the same redshift dependence as cold dark matter and baryons. This leaves density perturbations in the total matter δ_m and CDM + baryon δ_{cb} fields as ways to probe neutrino mass at low redshifts. So the success of upcoming surveys measuring neutrino mass hinges on their ability to measure the effects of neutrinos on the total matter and CDM + baryon perturbations, as well as on their ability to measure Ω_m from the redshift-distance relation (which can also be extracted from perturbations, such as from baryonic acoustic oscillations).

On large scales, neutrinos cluster analogously to CDM, whereas on small scales they do not cluster. The scale at which this transition occurs is known as the free streaming scale and is due to the neutrino thermal velocities erasing their own perturbations. We can thus divide perturbations into scales larger than the neutrino free streaming scale, where $\delta_\nu \sim \delta_{cb}$, and scales smaller than that, where $\delta_\nu \sim 0$. One can see that if one could measure δ_m and δ_{cb} on small scales in the absence of noise, then any difference between the two would give strong constraints on neutrino mass via $\delta_m \sim (1 - f_\nu)\delta_{cb}$. However, this poses several observational difficulties.

A first difficulty is that the matter overdensity field δ_m is not directly observable. weak-lensing probes the convergence, given by

$$\kappa(\chi_*, \hat{\boldsymbol{n}}) = \frac{3H_0^2\Omega_m}{2c^2}\int_0^{\chi_*} d\chi \frac{\chi}{a(\chi)}\left(1 - \frac{\chi}{\chi_*}\right)\delta_m(\chi\hat{\boldsymbol{n}}), \quad (3)$$

where χ is the comoving distance, χ_* is the comoving distance to the source, $\hat{\boldsymbol{n}}$ is the direction on the sky, H_0 is the Hubble constant, c is the speed of light, $a(\chi)$ is the expansion factor, and we assume zero curvature. Hence, κ can be viewed as a measurement of $\Omega_m\delta_m$ averaged over a radial window along the line of sight between the observer and the source. This dilutes the information contained in the total matter field.

A second issue is that we also cannot measure δ_{cb} directly. What we can typically measure from galaxy observations is a biased version, where at the linear level we have $\delta_g = b_1\delta_{cb}$, with galaxy overdensity δ_g being modulated by the linear bias b_1. The linear bias is constant on large scales, but has complicated scale dependence on small scales which cannot be predicted *ab initio*, and thus has to be marginalized over to obtain constraints on cosmological parameters. One way to measure it is using redshift-space distortions, which at the linear order probe density-velocity correlations. Velocity can be related to the matter overdensity via $\delta_v = f\delta_m$, where f is the linear growth rate that depends on the matter density Ω_m. The growth rate is also affected by neutrinos, which slow down the growth of structure on small scales. However, on small scales, i.e., beyond linear order, this relation also becomes more complicated due to higher-order velocity-density correlators (see, e.g., [13]), once again making it difficult to isolate the effects of neutrino mass.

Multitracer analyses, combining δ_g from spectroscopic or photometric surveys, with weak lensing κ from the cosmic microwave background (CMB) or large-scale structure (LSS), suggest that LSS surveys have the power to separate neutrino mass from other parameters and that sampling variance cancellation is helpful on large scales [14,15]. Nevertheless, this approach is limited to about 20 meV precision on the sum of neutrino masses for surveys such as LSST, suggesting it may not be able to give a neutrino mass detection at more than 3σ for the minimum theoretical mass of 60 meV.

This limited precision from multitracer probes has revived interest in measuring neutrinos from a single tracer using nonlinear information. By studying the nonlinear effects of massive neutrinos on structure formation [16–43], several such statistics have been proposed, including the bispectrum, halo mass function, void size function, probability distribution function, and marked power spectrum [44–55]. The reasoning is that a single tracer may have access to different types of information in different density regions. For example, while high density regions may be mostly sensitive to the CDM + baryons, which cluster and gravitationally collapse into virialized objects, low density regions such as voids may be more sensitive to neutrinos, which cluster weakly in comparison. Crucially, this implies that a full description of the system requires a two-fluid model, that of CDM + baryons and of neutrinos, which cannot be mimicked by a single CDM + baryon component. The hope of this approach is that, by effectively combining information from different density regimes, one might be able to determine neutrino mass to a much higher precision than predicted by just the two-point statistics, the power spectrum.

The goal of this paper is to investigate this single tracer proposal by comparing a single-fluid CDM simulation to a two-fluid simulation with CDM and neutrinos (for the purpose of this paper, we assume baryons trace CDM). We examine whether the presence of massive neutrinos has a unique *nonlinear* effect that differentiates the two at late times, or if the impact of the massive neutrino component can be faked by a solitary CDM component. To this end, we set up the two simulations with a matched linear power spectrum of the field in question and equal phases, at a redshift of interest, which we will take to be $z = 0$. We compare the two simulations at the field level for three different fields: (i) δ_{cb}, which uniquely defines anything observable with galaxies, (ii) $\Omega_m\delta_m$, which is the corresponding field controlling weak-lensing observables, and (iii) δ_m, the 3D total matter field, which is not currently observable.

If at the field level the two simulations differ in their phases at $z = 0$, this would suggest there is information that

has been created by the nonlinear evolution that is unique to the presence of massive neutrinos and that cannot be mimicked by a single CDM fluid. If, on the other hand, the final phases are matched exactly, then there is no information associated with the difference in nonlinear evolution beyond the overall amplitude of the field, i.e., the power spectrum. If the power spectra at $z = 0$ are also identical between the two simulations, then there is no nonlinear information arising specifically from the presence of the neutrino component, and any information regarding neutrino mass must simply arise from the differing linear physics. A similar analysis was performed in the context of modified gravity in [56], which studied only the nonlinear power spectrum. Earlier work in the context of neutrino mass includes a study of the halo mass function [57] and the nonlinear matter power spectrum for the Ly-α forest [58]. We will generalize such analyses by considering the information at the field level.

The structure of this paper is as follows. In Sec. II, we outline how to study the information content of cosmological fields. In Sec. III, we apply this to understand the amount of neutrino mass information in the various aforementioned cosmological fields. In Sec. IV, we then comment on the benefits of probes beyond the power spectrum (for example, related to halos and voids). In Sec. V, we consider a Fisher analysis to compare constraints obtained from the linear and nonlinear power spectrum. Finally, in Sec. VI, we conclude and discuss how our findings relate to constraints on M_ν presented in recent works.

II. COSMOLOGICAL INFORMATION

The simplest tool used to quantify the information content of a field $\delta(\boldsymbol{k})$ is the (auto)power spectrum $P_{\delta\delta}(k)$, defined via

$$\langle \delta^*(\boldsymbol{k})\delta(\boldsymbol{k}')\rangle = (2\pi)^3 P_{\delta\delta}(k)\delta^{(D)}(\boldsymbol{k}-\boldsymbol{k}'), \tag{4}$$

where $\delta^{(D)}$ is the Dirac delta function. $P_{\delta\delta}(k)$ is the Fourier transform of the two-point correlation function $\xi(r)$; i.e., it measures the overdensity correlation between two arbitrary points of space separated by r. For a statistically homogeneous, isotropic, and Gaussian field, the power spectrum contains the entire information of the field. The standard model of cosmology assumes homogeneity and isotropy and that the primordial Universe was described by a Gaussian random field (although we note that there are some extensions beyond this theory, for example, positing primordial non-Gaussianity [59–65]). The overdensity field in Fourier space is, in general, complex; i.e., it can be written as $\delta(\boldsymbol{k}) = |\delta(\boldsymbol{k})|e^{i\phi(\boldsymbol{k})}$, where $|\delta(\boldsymbol{k})|$ is the magnitude and $\phi(\boldsymbol{k})$ is the phase. The phases of a Gaussian random field have a uniform random distribution in the range $[0, 2\pi)$.

The Universe then evolves and, during the late stages of evolution, structure formation introduces non-Gaussianities on small scales due to the nonlinear nature of gravitational collapse. The exact nature of this nonlinear evolution depends on the cosmological parameters, for example, the energy density of dark energy Ω_Λ, the Hubble constant H_0, and the total neutrino mass M_ν. There is thus much interest in studying higher-order statistics, in the hope that they contain additional information beyond the power spectrum. This is particularly true in the case of neutrinos due their signature on small, nonlinear scales. It is thus important to understand how much information neutrinos imprint on different cosmological fields and, furthermore, how much of this information arises from nonlinear cosmic evolution.

To set up the problem, let us consider two different universes at some late redshift z_f. We denote some generic field as $\delta_X(\boldsymbol{k}, z_f)$ in the first universe with cosmological parameters λ and $\tilde{\delta}_X(\boldsymbol{k}, z_f)$ in the second universe with cosmological parameters $\tilde{\lambda}$. A question of interest is, if our Universe corresponds to δ, how well can we distinguish it from a universe with field $\tilde{\delta}$? Or, in other words, how much information can we learn about the cosmological parameters by studying $\delta(\boldsymbol{k}, z_f)$? While a typical analysis, e.g., a Fisher analysis, considers both linear and nonlinear information as one, we seek to isolate the nonlinear information. More concretely, while a cosmological field may be sensitive to a change in cosmological parameters, if this sensitivity is purely at the linear level, then there will be no additional information compared to the linear power spectrum; one could consider nonlinear probes, such as the halo mass function, void size function, the bispectrum, etc., but they will just be expressing the information content of the linear power spectrum in a different form. So it is interesting to study how much nonlinear information there is and thus how much benefit one can expect to extract from nonlinear observables.

To quantify how much nonlinear information an entire field contains with regard to a change in cosmological parameters $\lambda - \tilde{\lambda}$, we match the linear physics at z_f between the two cosmologies. We then backscale the fields to some earlier redshift z_i using linear theory twice: one time using the cosmology associated with λ and one time using $\tilde{\lambda}$. Finally, we perform an N-body simulation to evolve the two fields to z_f and obtain nonlinear results: here again we use the appropriate choice of cosmology in each case. A schematic of these two simulations is as follows:

$$\delta_X^{(1)}(z_f) \underset{\text{backscale}}{\overset{\lambda}{\hookrightarrow}} \delta_X^{(1)}(z_i) \underset{N-\text{body}}{\overset{\lambda}{\Rightarrow}} \delta_X(z_f), \tag{5}$$

$$\delta_X^{(1)}(z_f) \underset{\text{backscale}}{\overset{\tilde{\lambda}}{\hookrightarrow}} \tilde{\delta}_X^{(1)}(z_i) \underset{N-\text{body}}{\overset{\tilde{\lambda}}{\Rightarrow}} \tilde{\delta}_X(z_f), \tag{6}$$

where $\delta_X^{(1)}$ labels the linear power spectrum of component X. The key difference between this approach and a typical

analysis is the use of identical initial conditions for both universes to ensure the linear physics is the same at z_f after running the simulation. This means that any difference between $\delta_X(z_f)$ and $\tilde{\delta}_X(z_f)$ after the N-body simulation will be purely due to nonlinear effects caused by using $\tilde{\lambda}$ instead of λ.

Having set up the problem, we now review how to quantify the difference between two fields. Rather than considering specific observables, we seek to study effects at the field level. In order to compare the two fields at z_f, we consider the (complex) coherence of the two fields, defined as

$$\zeta(k) = \frac{P_{\delta\tilde{\delta}}(k)}{\sqrt{P_{\delta\delta}(k)P_{\tilde{\delta}\tilde{\delta}}(k)}}, \tag{7}$$

where $P_{\delta\tilde{\delta}}(k)$ is the cross-power spectrum between δ and $\tilde{\delta}$, given by

$$\langle \delta^*(\boldsymbol{k})\tilde{\delta}(\boldsymbol{k}')\rangle = (2\pi)^3 P_{\delta\tilde{\delta}}(k)\delta^{(D)}(\boldsymbol{k}-\boldsymbol{k}'). \tag{8}$$

Unlike the autopower spectrum, the cross-power spectrum can, in general, be complex. Note that statistical isotropy and homogeneity enforces the coherence to only be a function of the magnitude k.

Two fields are said to be *coherent* at scale k if $|\zeta(k)| = 1$. In such a case, the power spectra of the two fields are linearly related as follows:

$$P_{\tilde{\delta}\tilde{\delta}}(k) = \left|\frac{P_{\delta\tilde{\delta}}(k)}{P_{\delta\delta}(k)}\right|^2 P_{\delta\delta}(k), \tag{9}$$

where the $|\cdot|^2$ term can be thought of as a linear transfer function between the autospectra of the two fields.

If the real part of the coherence is equal to 1, the phases of δ and $\tilde{\delta}$ are statistically identical. If the phases of the two cosmologies evolved identically, then the entire difference between the two fields is captured by any difference in the amplitude of the individual power spectra. Furthermore, if two fields are coherent, and the transfer function is identical to unity, $|P_{\delta\tilde{\delta}}(k)/P_{\delta\delta}(k)| = 1$, this implies that the power spectra are identical and that there is thus no nonlinear information in the power spectrum. In such a case, the two cosmologies are statistically indistinguishable in terms of nonlinear effects, and there will be no information beyond the linear power spectrum. By this we mean that, for a given set of scales, the information content of any nonlinear statistic cannot exceed the information content of the linear power spectrum over those same scales. While the linear power spectrum is not something one can generally observe for a particular field, it is useful to know whether or not there is information that exists beyond linear theory.

III. MASSIVE NEUTRINO INFORMATION

Using the notation of the previous section, we use λ to denote a universe with massive neutrinos, $M_\nu = 0.15$ eV, and $\tilde{\lambda}$ to denote a universe without massive neutrinos, $M_\nu = 0$. We start by using a Boltzmann solver to compute the linear power spectrum for a cosmology with $M_\nu = 0.15$ eV at $z_f = 0$. We then backscale this power spectrum to $z_i = 99$ twice, one time using the linear physics associated with massive neutrinos (using the REPS package [66]), giving $P_X(k, z_i)$, and the other time using the linear physics associated with massless neutrinos, giving $\tilde{P}_X(k, z_i)$. We generate realizations of the two fields at $z = 99$ with matched phases. Note that the massless neutrino cosmology is thus initialized with a power spectrum whose shape encodes the linear suppression of growth due to the presence of massive neutrinos in the other cosmology. Then we evolve $P_X(k, z_i)$ through to z_f using the GADGET N-body simulation [67] with massive neutrinos, yielding $\delta_X(\boldsymbol{k}, z_f)$, and we similarly evolve $\tilde{P}_X(k, z_i)$ through to z_f using the N-body simulation without massive neutrinos, yielding $\tilde{\delta}(k, z_f)$. Since the linear predictions of the two cosmologies have been matched as closely as possible, we can determine how much nonlinear evolution is special to the presence of massive neutrinos by comparing the fields at z_f: $\delta(\boldsymbol{k}, z_f)$ and $\tilde{\delta}(\boldsymbol{k}, z_f)$. Furthermore, by comparing the power spectra of the fields $P_{\delta\delta}(k, z_f)$ and $P_{\tilde{\delta}\tilde{\delta}}(k, z_f)$, we can assess the information in the power spectrum. We refer to the $M_\nu > 0$ simulation as the "real" simulation and the $M_\nu = 0$ simulation as the "fake" simulation, because the purpose of the $M_\nu = 0$ simulation is to fake the effects of massive neutrinos by using a single-fluid CDM simulation with initial conditions associated with a massive neutrino cosmology. Note that, for each considered field δ_X, a different fake N-body simulation is run with matched linear physics for that particular field. We consider a box of volume 1 $(\mathrm{Gpc}/h)^3$ and a grid of dimension 1024^3 for both CDM and neutrinos.

In the case of lensing, the field δ_m is not directly measured. Instead, lensing measures $\Omega_m\delta_m$ averaged over a window function integrated over the line of sight, as described in Eq. (3). We are therefore free to define the effective lensing field by rescaling by a constant factor, which we choose to be $(1 - f_\nu)$ as follows:

$$\kappa \sim \Omega_m\delta_m = \Omega_m(1-f_\nu)\frac{\delta_m}{(1-f_\nu)} = \Omega_c\frac{\delta_m}{(1-f_\nu)}. \tag{10}$$

Assuming no *a priori* information regarding Ω_m, we can evaluate the lensing information by considering the information in the field defined by

$$\delta_{\Omega m} \equiv \frac{\delta_m}{(1-f_\nu)}. \tag{11}$$

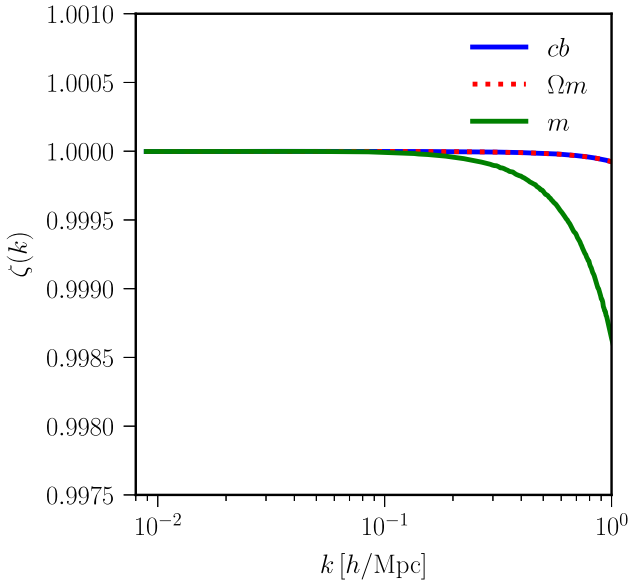

FIG. 1. The real part of the coherence between fields from the real and fake simulations. If we match δ_X at $z = 0$, we plot the coherence for δ_X. It can be seen that the coherence in the case of δ_{cb} and $\delta_{\Omega m}$ is one up to $k = 1\ h/\mathrm{Mpc}$ to $\lesssim 0.01\%$. This implies that there is negligible nonlinear information in the cb field or the lensed matter field at these scales that goes beyond the power spectrum. On the other hand, the coherence for δ_m begins to differ from one at a lower value of k, implying nonlinear information beyond the power spectrum for the 3D matter field.

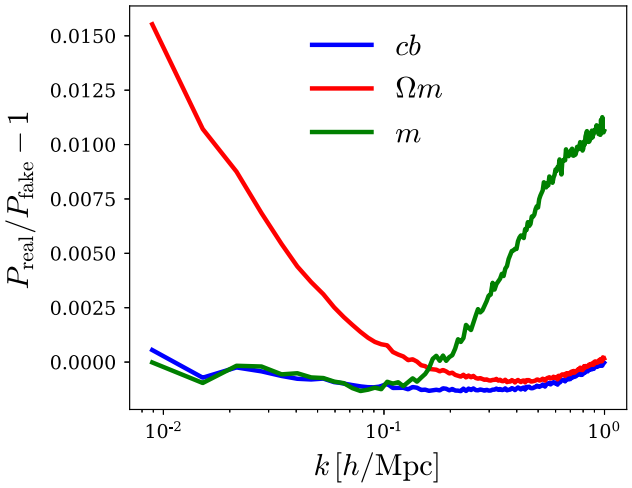

FIG. 2. The ratio of the power spectra between the real and fake simulations. If we match δ_X at $z = 0$, we plot the corresponding power spectrum P_X. It can be seen that the ratio is 1 for cb, while there is an approximately 1% deviation for $P_{\Omega m}$ on large scales. Only P_m differs from 1 on nonlinear scales, implying information beyond the power spectrum in for the matter field. In the cases of cb and Ωm, the $\lesssim 0.1\%$ upturn on scales smaller than $k \approx 0.5\ h/\mathrm{Mpc}$ is a numerical artifact due to discrepancy between the backscaling and forward model; a similar effect can be seen in the case of m for which a downturn begins at $k \approx 0.5\ h/\mathrm{Mpc}$.

While we are free to choose any normalization, the reason for this choice is that we seek the option that most closely matches the real and fake cosmologies. From Eq. (2) it is clear that $\delta_{\Omega m} \sim \delta_{cb}$ on small scales, thus this choice is inspired such that neutrino effects should be negligible on small scales (note that in the case of $\delta_{\Omega m}$ linear matching cannot be achieved at large scales, but rather on small scales).

In Fig. 1 we plot the real part of the coherence for each of the fields between the real and fake simulations. Specifically, when we match P_X at $z = 0$, we plot the coherence for the X overdensity field. It can first be seen that, in the case of $X = cb$, the coherence is unity up to $k = 1\ h/\mathrm{Mpc}$ to $\lesssim 0.01\%$. This implies that the final phases of the cb field are equivalent regardless of whether massive neutrinos are included in the simulation. This is to say that the nonlinear evolution of the cb field is identical in both the one-fluid (CDM) and two-fluid (CDM + ν) description. Thus, there is negligible nonlinear information in the cb field that goes beyond the power spectrum within scales of experimental interest. On the other hand, the coherence for δ_m begins to differ from 1 at a lower value of k, implying there is nonlinear information beyond the power spectrum for the 3D matter field. However, one cannot measure the matter field directly, and one instead measures lensing that is related to $\delta_{\Omega m}$, as in Eq. (11). In this case, the picture is identical to δ_{cb}, with a coherence of 1 up to $k = 1\ h/\mathrm{Mpc}$ to $\lesssim 0.01\%$, implying negligible nonlinear information beyond the power spectrum in this field at these scales.

Having established that, for scales of interest, the information in the case of δ_{cb} and $\delta_{\Omega m}$ is all in the power spectrum, we now consider how much information the power spectrum contains. In Fig. 2 we plot the ratio between the power spectra for the various fields at redshift z_f. We see that for P_{cb} the ratio is always one, implying that there is negligible nonlinear information regarding neutrinos in the cb power spectrum. (We note that the $\lesssim 0.1\%$ upturn for scales smaller than $k \approx 0.5\ h/\mathrm{Mpc}$ is a numerical artifact caused by a slight discrepancy between the growth factor implemented in backscaling and that effectively implemented by the N-body simulation. The magnitude of this discrepancy depends on M_ν, leading to this small effect.) Given the coherence of the cb field is one, this means there is negligible nonlinear information about neutrino mass in the entire cb field. On the other hand, there is a deviation of order 1% in $P_{\Omega m}$ for $k \lesssim 0.1\ h/\mathrm{Mpc}$. This implies there is some information on neutrino mass in the lensed matter power spectrum. This is the typical shape information associated with neutrinos; however, it mostly appears on large, linear scales and will thus be sample variance limited. Finally, we see that the ratio for P_m differs from one on small scales, implying the presence of nonlinear information about neutrinos beyond the linear power spectrum of the 3D total matter field.

To summarize, whenever we consider the single-fluid CDM field, we find that there is no difference between the

real and fake simulations. On the other hand, whenever we consider fields that explicitly depend on both fluids (CDM + ν) in the real simulations, we generally find that a single fake simulation cannot reproduce the statistics on all scales: either they remain matched on large scales, or they remain matched on small scales. The two choices we explore, m and Ωm, illustrate this clearly. For m, the small scales have a different nonlinear behavior even though the linear statistics are exactly matched. For Ωm, the large scales are not matched even at the linear level, but crucially, the small-scale matching is maintained both at the linear and nonlinear level. Since for Ωm only the linear scales are not matched well, most of the information should be contained in the linear power spectrum.

IV. HIGHER-ORDER STATISTICS

We now illustrate the effect of the results of the previous section on various statistics beyond the power spectrum. While the results of the previous section are sufficient in determining the presence of information regarding M_ν in any nonlinear statistic beyond the power spectrum, we now show this explicitly for various examples in the interest of clarity.

We start with the void size function (VSF), a commonly proposed source of information regarding neutrino mass [44]. We use the spherical void finder of [29] with a threshold of $\delta_{\rm th} = -0.7$ and look for voids in the three considered fields: cb, Ωm, and m. In Fig. 3 we find that there is no difference in the VSF between the real and fake simulations for both the cb and Ωm fields, but there is potentially some difference for the 3D matter field. Note that we find similar results regardless of the value of $\delta_{\rm th}$.

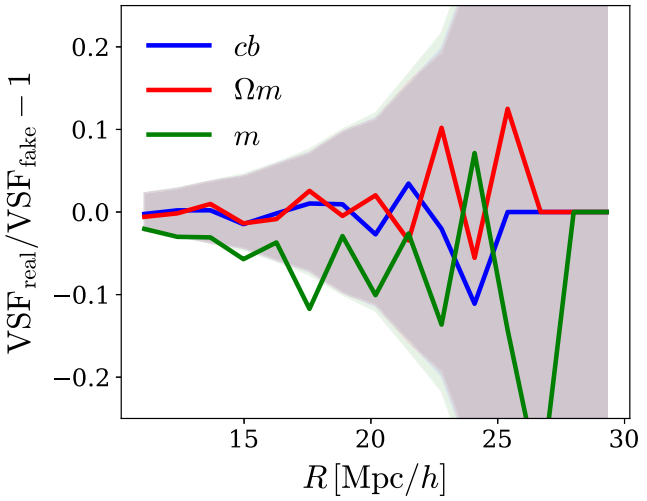

FIG. 3. The ratio of the void size function between the real and fake simulations. If we match δ_X at $z = 0$, we plot the corresponding VSF in the X field. Bands represent Poisson errors. It can be seen that the ratio is 1 for cb and Ωm within the Poisson errors. Only the VSF in the 3D matter field shows a ratio that is not unity, although it is still close to the Poisson error.

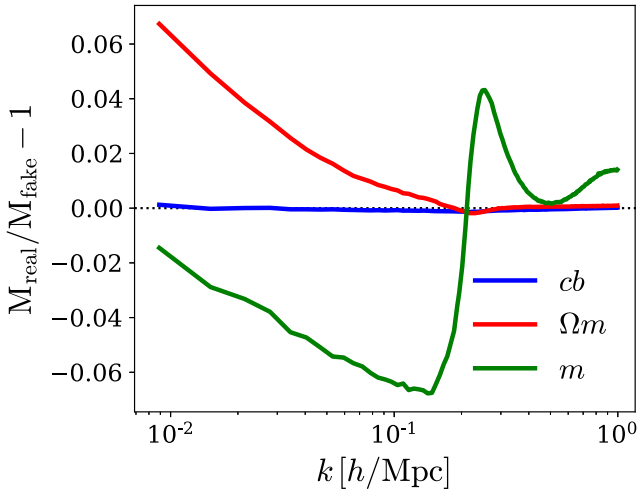

FIG. 4. The ratio of the marked power spectrum (M) between the real and fake simulations. If we match δ_X at $z = 0$, we plot the corresponding M in the X field. It can be seen that the ratio is 1 for cb, while for the Ω_m it deviates from 1 on large scales, and for m is deviates from 1 on all scales.

Next, in Fig. 4, we consider the marked power spectrum. We use the optimal choice of mark parameters found in [53], which uses the smoothed overdensity field with 10 Mpc/h smoothing window; thus small-scale information is mixed into large scales. We again find little difference in the cb field. The Ωm field differs only on large, linear scales. For the m field, there is a difference on all scales. Again, this fits with our findings in the previous section.

A corollary of there being negligible information in the cb field is that there will also be negligible information in the halo field. The halo field is a function of the cb field and the bias parameters; hence, without knowledge of the bias, the information content of the halo field is just a reexpression of the information contained in the cb field. We illustrate this in Fig. 5, which shows the difference in the power spectrum, void size function, and marked power spectrum, for the halo field between the real and fake (cb-matched) simulations. We identify halos using the friends-of-friends algorithm and apply a fixed number density cut. We find that there is no significant difference in any of the halo statistics between the real and fake simulations.

Having shown there to be little information in the real-space halo field, we now consider redshift-space distortions (RSDs), which include the effects of the peculiar velocities of halos along the line of sight (LOS). The peculiar velocity field is sourced by the clustering of the total matter field, which includes neutrinos. The halo power spectrum in redshift space can, therefore, provide additional information on the total neutrino mass. In the left panel of Fig. 6, we show a bin-by-bin comparison of the redshift-space halo power spectrum from the real and fake (with matched cb field) simulations in the $(k_\parallel, k_\perp)$ plane, where parallel/

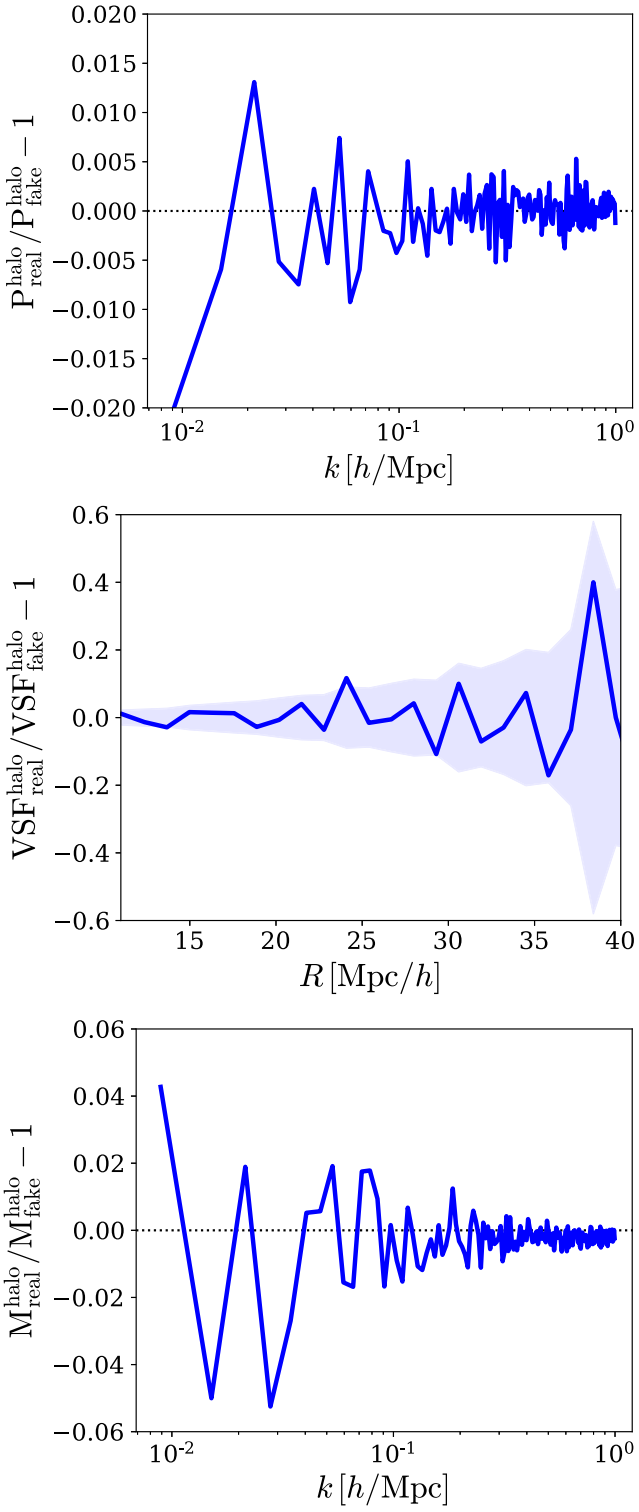

FIG. 5. The ratio of the halo-traced power spectrum, void size function, and marked power spectrum (from top to bottom) between the real and fake (cb-matched) simulations. It can be seen that the ratio is close to unity in all cases.

perpendicular is in reference to the LOS. It can be seen that some bins along the LOS have a relatively large difference between the two simulations, but even small deviations from the LOS direction bring the size of the effect down to $\lesssim 1\%$, in line with the results obtained in real space. To better visualize the dependence on magnitude k and projection onto the LOS, $\mu = k_{\parallel}/k$, we bin the data into three bins of k and four bins of μ. The right panel shows the difference between the real and fake simulation increases with k and μ, signifying the information present at small scales due to RSDs as one approaches the LOS. Therefore, we conclude that there is indeed additional nonlinear information about neutrino mass that can be obtained by studying clustering of biased tracers in redshift space. While this clustering can be difficult to model accurately, it may be a key source of information in upcoming surveys [68].

V. FISHER ANALYSIS

As shown the previous two sections, without RSDs, the cb field is statistically indistinguishable between the one-fluid (CDM) and two-fluid (CDM+ν) simulations. The same is also approximately true for the Ωm field, responsible for weak lensing, for which there is only a difference in the power spectrum on large scales. If there is negligible difference between the one-fluid and the two-fluid nonlinear dynamics, the total information content is essentially maximized by that which arises from the linear physics. Nevertheless, as the linear power spectrum is not observable, it is instructive to compare the information content of the linear power spectrum to the nonlinear power spectrum.

We perform a Fisher analysis in the $\{\Omega_m, \Omega_b, h, n_s, \sigma_8, M_\nu\}$ plane. We use a fiducial cosmology with $\Omega_m = 0.3175$, $\Omega_b = 0.049$, $h = 0.6711$, $n_s = 0.9624$, $\sigma_8 = 0.834$, and $M_\nu = 0.05$ eV. To compute derivatives, we use a central difference scheme at $\pm\delta\theta$ for each cosmological parameter. Specifically, we use $\delta\Omega_m = 0.01$, $\delta\Omega_b = 0.002$, $\delta h = 0.02$, $\delta n_s = 0.02$, $\delta\sigma_8 = 0.015$, and $\delta M_\nu = 0.025$ eV. For the linear covariance between probes x and y, we use $C_X = 2P_X^2/N_k$, where $N_k = 4\pi k^2 k_F/k_F^3$, and $k_F = 2\pi/L$ is the fundamental wave number, which we take for a box of volume 1 $(\mathrm{Gpc}/h)^3$. For the nonlinear results, we use the QUIJOTE simulations [69], and for the linear results we use CAMB [70], using the same derivative computation method and binning as QUIJOTE.

Figure 7 shows the marginal error on M_ν as a function of k_{max} for the various linear and nonlinear power spectra. As expected,there is good agreement between the linear and nonlinear results on large scales, where cosmic evolution is approximately linear. Moving to smaller scales, we see that the nonlinear power spectra for cb and Ωm have a factor 2 times lower constraining power compared to their linear counterparts. Note that the nonlinear power has worse constraints because its covariance has positive off-diagonal elements due to mode coupling, which in turn degrades the information content after marginalizing [54]. This means that there is still potential room for improvement upon the constraints from the nonlinear power spectrum, and one

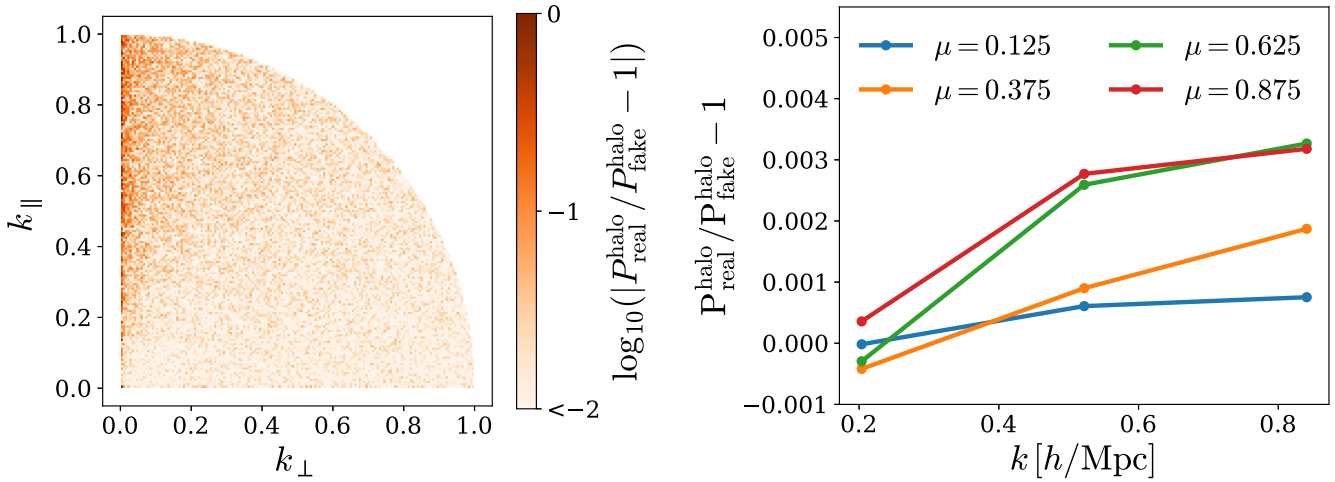

FIG. 6. The ratio of the redshift-space halo power spectrum between the real and fake (cb-matched) simulations. Left: bin-by-bin comparison in the $(k_\parallel, k_\perp)$ plane, where parallel/perpendicular is in reference to the LOS. Right: binning the data into three bins of magnitude k and four bins of LOS projection, $\mu = k_\parallel/k$. Both plots show a deviation of the ratio from unity when moving closer to the LOS and to smaller scales, but negligible deviation in the perpendicular direction, suggesting that the additional information on neutrino mass comes from the modified velocity field, or growth rate, which is sourced by the matter overdensity.

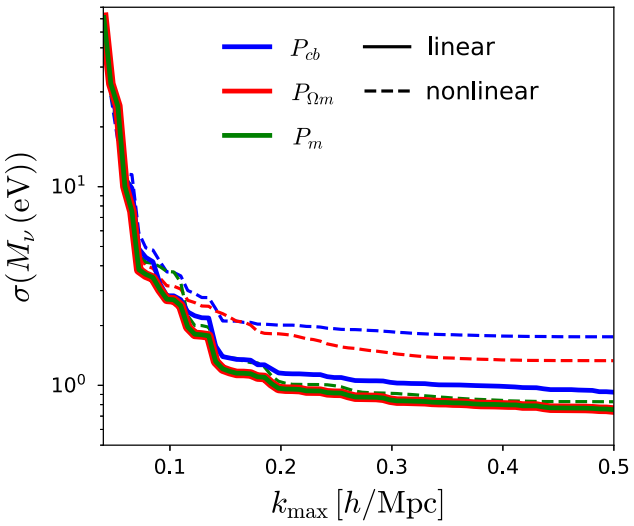

FIG. 7. Marginal error on M_ν for P_{cb} (blue), $P_{\Omega m}$ (red), and P_m (green), in both the linear (solid) and nonlinear (dashed) regime, for a volume of 1 $({\rm Gpc}/h)^3$.

may benefit from around a factor 2 by using statistics beyond the power spectrum. Thus, on their own, the cb and Ωm fields give a marginal error on the neutrino mass of just under 1 eV in a 1 $({\rm Gpc}/h)^3$ volume.

On the other hand, the linear and nonlinear marginal error on P_m match well all the way to $k_{\rm max} = 0.5\ h/{\rm Mpc}$. But, regardless of this, it was shown in the previous section that there is additional information in the phases of the 3D matter field that is not fully captured by the power spectrum, and there is thus additional information to be found in higher-order statistics.

VI. DISCUSSION AND CONCLUSIONS

In this paper we have investigated how much nonlinear information regarding neutrino mass one can expect to find in various cosmological fields by comparing one-fluid (CDM) to two-fluid (CDM + ν) simulations with matched initial conditions. In real space, we found that the cb field and Ωm (lensing) field do not contain additional information regarding neutrino mass that is unique to the two-fluid dynamics up to $k \lesssim 1\ h/{\rm Mpc}$. Essentially, the evolutionary effect of including a massive neutrino fluid can be faked by a solitary CDM fluid. This implies that the cb field and derived quantities (e.g., the halo field) and weak-lensing convergence, contain little information regarding neutrino mass beyond that which exists in the linear power spectrum over the same scales. We have also shown that there is much nonlinear information regarding neutrino mass in the 3D matter overdensity field; however, this is not currently experimentally detectable. The fundamental quantities we considered are the coherence and power spectrum ratio between the two simulations, summarized in Table I, which alone quantify the amount

TABLE I. Summary of key results. The coherence and power spectrum ratio between the real and fake simulations for the cb, Ωm, and m fields, for $k \le 1\ h/{\rm Mpc}$. Note that, while the power spectrum ratio for the Ωm field differs from unity at the 1% level, this is only at low k, which is sample variance limited.

Field	$\zeta - 1$	$P_{\rm real}/P_{\rm fake} - 1$
cb	$\lesssim$0.01%	$\lesssim$0.1%
Ωm	$\lesssim$0.01%	$\lesssim$1% (low k)
m	$\lesssim$0.1%	$\lesssim$1%

of nonlinear information at the field level. We then explicitly verified these findings for various higher-order statistics, including the void size function and marked power spectrum.

Consequently, one can expect constraints on neutrino mass a little lower than 1 eV in a volume of 1 $(\mathrm{Gpc}/h)^3$ when using the cb or lensing fields alone at a single redshift. Hence, using only this information, a very large volume of 10^4 $(\mathrm{Gpc}/h)^3$ would be needed to reach an error of 0.01 eV (corresponding to a $\sim 5\sigma$ detection), which exceeds the available volume of currently realistic surveys.

We note that, even in the face of these findings, there is still motivation to consider statistics beyond the power spectrum to detect neutrino mass. A first consideration is the choice of redshift(s). In our analysis, we have matched the linear physics at a single redshift, $z = 0$. Similarly, [58] used hydrodynamical simulations to find that one can fake the effects of massive neutrinos in the nonlinear power spectrum up to $k \lesssim 10/\mathrm{Mpc}$ for the Ly-α forest ($z = 3$). While the effects of massive neutrinos can be faked at a single redshift, the real and fake universes have, in principle, different evolution. Therefore, combining the fields at multiple redshifts should help discriminate between the two and improve constraints on M_ν. It will thus be imperative to combine multiple redshifts (from CMB redshift of 1100 to today) and tracers (CMB, galaxies, and weak lensing) to obtain tight constraints on neutrino mass in upcoming surveys. For example, combining weak lensing and galaxy clustering, can reach 0.02 eV with Rubin (LSST) and stage IV CMB [14].

Second, the late-time linear power spectrum is not an observable quantity, as cosmic evolution is indeed nonlinear. Hence, even though the linear power spectrum may provide a bound for the error in the case of cb and lensing, the nonlinear power spectrum does not quite reach this bound. We have shown this effect corresponds to around a factor of 2, thus a different nonlinear statistic may be able to obtain slightly better constraints than the nonlinear power spectrum. This factor of 2 can also be recovered by reconstructing the linear field from the nonlinear field [71].

Third, we consider lensing measurements to be directly sensitive to the product $\Omega_m\delta_m$. This is exact if the sources are at low redshift. However, the comoving distance in Eq. (3) implicitly depends on Ω_m as well, so for sources at higher redshift the relation is more complicated. Thus, all possible combinations of Ω_m and δ_m that keep $\Omega_m\delta_m$ fixed may not be compatible with the observed lensing signal because they will modify the comoving distances. If one could obtain strong constraints on Ω_m from the redshift-distance relation, then combining it with lensing measurements may be able to probe δ_m directly, rather than the product $\Omega_m\delta_m$. We also note that neutrinos are nonrelativistic at low redshift and thus will not induce a significant geometric effect on lensing observables that is known to arise in the context of dark energy [72,73].

Fourth, we have motivated that RSDs may provide nonlinear information regarding neutrino mass, thus considering higher-order statistics in redshift space is a worthwhile pursuit. RSDs add new information because velocities are determined by the growth factor f, which is sensitive to matter density Ω_m and neutrino density Ω_ν. While RSDs can be difficult to model, it could be a key source of information in upcoming surveys [68]. For example, [74] illustrates how halo velocities can aid in constraining neutrino mass. A further improvement on f may be possible from redshift dependence, which we did not consider in this paper.

Fifth, it might be argued that even for the cb or Ωm fields one could find information regarding M_ν beyond the linear power spectrum, as there may be a nonlinear statistic with more favorable parameter degeneracies. For example, a particular nonlinear statistic might constrain some other cosmological parameter much better than the linear power spectrum, and thus after marginalizing over this parameter, the constraints on M_ν will outperform the linear power spectrum. However, the other parameters of key relevance in the case of neutrino mass are Ω_m and A_s, for which nonlinear cosmic evolution does not induce additional information beyond that which exists in the linear initial conditions. We illustrate this in the Appendix. Thus, it is not expected that degeneracies will cause a big improvement in the constraints on M_ν. One could also consider nonstandard cosmological parameters, for example, related to primordial non-Gaussianity or exotic neutrino interactions [75]. For the latter to have an effect there would likely need to be a mechanism that couples the nonlinear evolutions of the cb and neutrino perturbations much more strongly than what happens through the Poisson equation. In principle, this is possible given a sufficiently strong neutrino-baryon or neutrino-neutrino interaction, and this could help break degeneracies with neutrino mass if one had a means to measure this nonstandard effect.

Numerous recent works have proposed that one can obtain information regarding neutrino mass beyond the power spectrum [45–55,76,77]. Some forecast $\mathcal{O}(0.1\ \mathrm{eV})$ constraints by employing tomography, which is in good agreement with our results. On the other hand, some works find constraints that are over an order of magnitude smaller than linear theory. Given our findings we are able to explain exactly where this information comes from. In the case of [50,51], the information arises from working in redshift space, while for [52–54] it comes from working with the 3D matter field. Regarding [55], which considers the real-space halo field, the information comes from assuming knowledge of the bias model as a function of cosmology. The bias model can be thought to transfer information on small scales in the cb field to larger scales in the halo field, thus information at $k > 1\ h/\mathrm{Mpc}$ in the cb field could move to scales of $k < 1\ h/\mathrm{Mpc}$ in the halo field. Hence, if one knew the bias model, one could obtain tight constraints

on the neutrino mass with modern measurements of the halo field. However, the bias model parameters can have strong degeneracies with the cosmological parameters; for example, the linear bias b_1 is essentially degenerate with σ_8. It is thus important to marginalize over bias and apply halo mass or number density cuts to obtain realistic constraints.

Many of the works that compute constraints on M_ν are based on Fisher forecasts, for which one must take great care to avoid inaccurate results [78–80]. Additionally, a Fisher analysis employs asymptotic limits using the Taylor expansion of the log likelihood, which may not be justified in a realistic data analysis where the posteriors are often non-Gaussian. Thus, while some practitioners do go to great lengths to show that their Fisher matrices have converged, it is unclear how credible such forecasts are for higher-order statistics. There is a growing trend in modern statistical inference and machine learning to use cross-validation as a golden standard for validation of results. The same standard should be adopted in cosmology as well. This means setting aside some fraction of simulations that are not used for training (i.e., not used to evaluate the covariance or derivatives of summary statistics) and performing an end-to-end analysis on these validation simulations all the way to the cosmological parameters of interest, where the result can be compared to the truth in terms of bias and variance. Such an analysis is expensive, even more so if the validation simulations are chosen to be produced by an independent simulation code, but this could be a worthwhile standard validation procedure. Another worthwhile verification strategy is to use null tests, in which one explicitly performs the analysis on setups where the signal is known to be null. An example is running non-Gaussian statistical analysis on Gaussian data to demonstrate that the Fisher analysis does not give more information than what is available in the Gaussian field. Thus, a useful piece of future work would be to train a neural network to learn the effects of massive neutrinos on the various cosmological fields and perform all of these tests. In the absence of such work, we intend for our results to give a useful rule of thumb when proposing new statistics to measure the nonlinear effects of massive neutrinos.

ACKNOWLEDGMENTS

We thank Francisco Villaescusa-Navaro for many insightful discussions on the manuscript. A. E. B. was supported by the Fermi Research Alliance, LLC under Award No. DE-AC02-07CH11359 with the U.S. Department of Energy and the U.S. Department of Energy (DOE) Office of Science Distinguished Scientist Fellow Program. This material is based upon work supported by the National Science Foundation under Grants No. 1814370 and No. 1839217 and by NASA under Grant No. 80NSSC18K1274. We acknowledge the use of CAMB for computations involving the linear power spectrum [70]. The QUIJOTE simulations [69] can be found at https://github.com/franciscovillaescusa/quijote-simulations. The analysis of the simulations has made use of the PYLIANS libraries, publicly available at https://github.com/franciscovillaescusa/Pylians3. Some of the computing for this project was performed on the Sherlock cluster. The authors would like to thank Stanford University and the Stanford Research Computing Center for providing computational resources and support that contributed to these research results.

APPENDIX: OTHER PARAMETERS (Ω_m AND A_s)

In this paper, we have studied the effect of neutrino mass M_ν on nonlinear cosmic evolution. We now briefly discuss the effects of two other cosmological parameters relevant for disentangling the effects of neutrino mass from large-scale structures: Ω_m and A_s.

We first perform the real-versus-fake analysis on the cosmological parameter Ω_m. We seek to test if nonlinear evolution leaves an imprint at the field level. To do so, we match the linear $P(k)$ of two $M_\nu = 0$ simulations, but differ the value of Ω_m by 10% between the two, during both backscaling and the forward N-body simulation. Figure 8 shows the coherence between these two simulations, which is shown to be $\lesssim 0.01\%$ for $k \lesssim 1h/\mathrm{Mpc}$. This suggests there is negligible additional information regarding Ω_m coming from the nonlinear evolution that would be present in higher-order statistics, since the agreement is exact at the field level. Interestingly, this is about the same value as the coherence

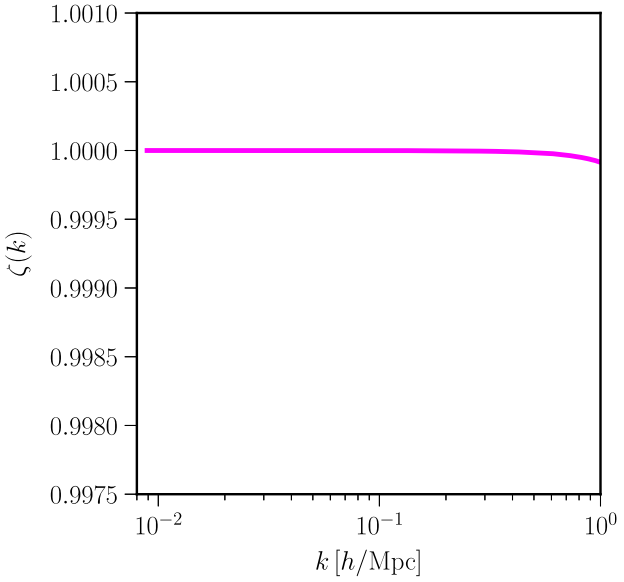

FIG. 8. The real part of the coherence between the cb fields from two $M_\nu = 0$ simulations with matched linear $P(k)$ at $z = 0$, but with Ω_m differing by 10%. It can be seen that the coherence is one up to $k = 1\ h/\mathrm{Mpc}$ to $\lesssim 0.01\%$. This implies that there is negligible nonlinear information regarding Ω_m in the cb field. The vertical range is identical to Fig. 1 to enable comparison.

found for the real-versus-fake M_ν coherence found in Fig. 1. Note that this analysis does not take into account any change in the shape of $P(k)$ due to a change in Ω_m, which is information contained in the initial conditions.

The other parameter of relevance when it comes to neutrino mass is the amplitude of linear fluctuations A_s. As this is the amplitude of the initial linear power spectrum, it is a property of the initial conditions. Thus, late-time nonlinear evolution cannot produce additional information on A_s.

We thus conclude that there is little information regarding M_ν, Ω_m, or A_s coming from nonlinear cosmic evolution. Hence, for $k \lesssim 1\ h/\mathrm{Mpc}$ in the cb or Ωm fields, there is no nonlinear statistic that will constrain these parameters significantly better than the linear power spectrum, even after marginalizing.

[1] https://www.desi.lbl.gov.
[2] https://www.euclid-ec.org.
[3] https://www.lsst.org.
[4] https://pfs.ipmu.jp/index.html.
[5] https://www.skatelescope.org.
[6] https://wfirst.gsfc.nasa.gov/index.html.
[7] J. Lesgourgues and S. Pastor, Massive neutrinos and cosmology, Phys. Rep. **429**, 307 (2006).
[8] Y. Fukuda, T. Hayakawa, E. Ichihara, K. Inoue, K. Ishihara, H. Ishino, Y. Itow, T. Kajita, J. Kameda, S. Kasuga *et al.*, Evidence for Oscillation of Atmospheric Neutrinos, Phys. Rev. Lett. **81**, 15621567 (1998).
[9] Q. R. Ahmad *et al.* (SNO Collaboration), Direct Evidence for Neutrino Flavor Transformation from Neutral Current Interactions in the Sudbury Neutrino Observatory, Phys. Rev. Lett. **89**, 011301 (2002).
[10] T. Araki *et al.* (KamLAND Collaboration), Measurement of Neutrino Oscillation with KamLAND: Evidence of Spectral Distortion, Phys. Rev. Lett. **94**, 081801 (2005).
[11] M. H. Ahn *et al.* (K2K Collaboration), Measurement of neutrino oscillation by the k2k experiment, Phys. Rev. D **74**, 072003 (2006).
[12] F. P. An *et al.*, Observation of Electron-Antineutrino Disappearance at Daya Bay, Phys. Rev. Lett. **108**, 171803 (2012).
[13] S.-F. Chen, Z. Vlah, E. Castorina, and M. White, Redshift-space distortions in lagrangian perturbation theory, J. Cosmol. Astropart. Phys. 03 (2021) 100.
[14] M. Schmittfull and U. Seljak, Parameter constraints from cross-correlation of CMB lensing with galaxy clustering, Phys. Rev. D **97**, 123540 (2018).
[15] B. Yu, R. Z. Knight, B. D. Sherwin, S. Ferraro, L. Knox, and M. Schmittfull, Towards neutrino mass from cosmology without optical depth information, arXiv:1809.02120.
[16] S. Saito, M. Takada, and A. Taruya, Impact of Massive Neutrinos on the Nonlinear Matter Power Spectrum, Phys. Rev. Lett. **100**, 191301 (2008).
[17] J. Brandbyge and S. Hannestad, Grid based linear neutrino perturbations in cosmological n-body simulations, J. Cosmol. Astropart. Phys. 05 (2009) 002.
[18] J. Brandbyge and S. Hannestad, Resolving cosmic neutrino structure: A hybrid neutrino n-body scheme, J. Cosmol. Astropart. Phys. 01 (2010) 021.
[19] M. Shoji and E. Komatsu, Massive neutrinos in cosmology: Analytic solutions and fluid approximation, Phys. Rev. D **81**, 123516 (2010); **82**, 089901(E) (2010).
[20] M. Viel, M. G. Haehnelt, and V. Springel, The effect of neutrinos on the matter distribution as probed by the intergalactic medium, J. Cosmol. Astropart. Phys. 6 (2010) 015.
[21] Y. Ali-Hamoud and S. Bird, An efficient implementation of massive neutrinos in non-linear structure formation simulations, Mon. Not. R. Astron. Soc. **428**, 3375 (2013).
[22] S. Bird, M. Viel, and M. G. Haehnelt, Massive neutrinos and the non-linear matter power spectrum, Mon. Not. R. Astron. Soc. **420**, 2551 (2012).
[23] S. Bird, Y. Ali-Hamoud, Y. Feng, and J. Liu, An efficient and accurate hybrid method for simulating non-linear neutrino structure, Mon. Not. R. Astron. Soc. **481**, 1486 (2018).
[24] M. Costanzi, F. Villaescusa-Navarro, M. Viel, J.-Q. Xia, S. Borgani, E. Castorina, and E. Sefusatti, Cosmology with massive neutrinos III: The halo mass function and an application to galaxy clusters, J. Cosmol. Astropart. Phys. 12 (2013) 012.
[25] F. Villaescusa-Navarro, F. Marulli, M. Viel, E. Branchini, E. Castorina, E. Sefusatti, and S. Saito, Cosmology with massive neutrinos I: Towards a realistic modeling of the relation between matter, haloes and galaxies, J. Cosmol. Astropart. Phys. 03 (2014) 011.
[26] F. Villaescusa-Navarro, A. Banerjee, N. Dalal, E. Castorina, R. Scoccimarro, R. Angulo, and D. N. Spergel, The imprint of neutrinos on clustering in redshift space, Astrophys. J. **861**, 53 (2018).
[27] E. Castorina, E. Sefusatti, R. K. Sheth, F. Villaescusa-Navarro, and M. Viel, Cosmology with massive neutrinos II: On the universality of the halo mass function and bias, J. Cosmol. Astropart. Phys. 02 (2014) 049.
[28] E. Castorina, C. Carbone, J. Bel, E. Sefusatti, and K. Dolag, Demnuni: The clustering of large-scale structures in the presence of massive neutrinos, J. Cosmol. Astropart. Phys. 07 (2015) 043.
[29] A. Banerjee and N. Dalal, Simulating nonlinear cosmological structure formation with massive neutrinos, J. Cosmol. Astropart. Phys. 11 (2016) 015.
[30] M. Archidiacono and S. Hannestad, Efficient calculation of cosmological neutrino clustering in the non-linear regime, J. Cosmol. Astropart. Phys. 06 (2016) 018.
[31] C. Carbone, M. Petkova, and K. Dolag, Demnuni: Isw, rees-sciama, and weak-lensing in the presence of massive neutrinos, J. Cosmol. Astropart. Phys. 07 (2016) 034.

[32] A. Upadhye, J. Kwan, A. Pope, K. Heitmann, S. Habib, H. Finkel, and N. Frontiere, Redshift-space distortions in massive neutrino and evolving dark energy cosmologies, Phys. Rev. D **93**, 063515 (2016).
[33] J. Adamek, R. Durrer, and M. Kunz, Relativistic n-body simulations with massive neutrinos, J. Cosmol. Astropart. Phys. 11 (2017) 004.
[34] J. D. Emberson, H.-R. Yu, D. Inman, T.-J. Zhang, U.-L. Pen, J. Harnois-Draps, S. Yuan, H.-Y. Teng, H.-M. Zhu, X. Chen *et al.*, Cosmological neutrino simulations at extreme scale, Res. Astron. Astrophys. **17**, 085 (2017).
[35] D. Inman and U.-L. Pen, Cosmic neutrinos: A dispersive and nonlinear fluid, Phys. Rev. D **95**, 063535 (2017).
[36] L. Senatore and M. Zaldarriaga, The effective field theory of large-scale structure in the presence of massive neutrinos, arXiv:1707.04698.
[37] H.-R. Yu, J. Emberson, D. Inman, T.-J. Zhang, U.-L. Pen, J. Harnois-Draps, S. Yuan, H.-Y. Teng, H.-M. Zhu, X. Chen *et al.*, Differential neutrino condensation onto cosmic structure, Nat. Astron. **1**, 0143 (2017).
[38] A. Banerjee, D. Powell, T. Abel, and F. Villaescusa-Navarro, Reducing noise in cosmological n-body simulations with neutrinos, J. Cosmol. Astropart. Phys. 09 (2018) 028.
[39] J. Liu, S. Bird, J. M. Z. Matilla, J. C. Hill, Z. Haiman, M. S. Madhavacheril, D. N. Spergel, and A. Petri, MassiveNuS: Cosmological massive neutrino simulations, J. Cosmol. Astropart. Phys. 03 (2018) 049.
[40] J. Dakin, J. Brandbyge, S. Hannestad, T. HaugbØlle, and T. Tram, νCONCEPT: Cosmological neutrino simulations from the non-linear Boltzmann hierarchy, J. Cosmol. Astropart. Phys. 02 (2019) 052.
[41] J. Z. Chen, A. Upadhye, and Y. Y. Y. Wong, One line to run them all: Supereasy massive neutrino linear response in n-body simulations, J. Cosmol. Astropart. Phys. 04 (2021) 078.
[42] J. Z. Chen, A. Upadhye, and Y. Y. Y. Wong, The cosmic neutrino background as a collection of fluids in large-scale structure simulations, J. Cosmol. Astropart. Phys. 03 (2021) 065.
[43] A. E. Bayer, A. Banerjee, and Y. Feng, A fast particle-mesh simulation of non-linear cosmological structure formation with massive neutrinos, J. Cosmol. Astropart. Phys. 01 (2021) 016.
[44] C. D. Kreisch, A. Pisani, C. Carbone, J. Liu, A. J. Hawken, E. Massara, D. N. Spergel, and B. D. Wandelt, Massive neutrinos leave fingerprints on cosmic voids, Mon. Not. R. Astron. Soc. **488**, 4413 (2019).
[45] J. Liu and M. S. Madhavacheril, Constraining neutrino mass with the tomographic weak lensing one-point probability distribution function and power spectrum, Phys. Rev. D **99**, 083508 (2019).
[46] Z. Li, J. Liu, J. M. Z. Matilla, and W. R. Coulton, Constraining neutrino mass with tomographic weak lensing peak counts, Phys. Rev. D **99**, 063527 (2019).
[47] W. R. Coulton, J. Liu, M. S. Madhavacheril, V. Böhm, and D. N. Spergel, Constraining neutrino mass with the tomographic weak lensing bispectrum, J. Cosmol. Astropart. Phys. 05 (2019) 043.
[48] G. A. Marques, J. Liu, J. M. Zorrilla Matilla, Z. Haiman, A. Bernui, and C. P. Novaes, Constraining neutrino mass with weak lensing Minkowski Functionals, J. Cosmol. Astropart. Phys. 6 (2019) 019.
[49] V. Ajani, A. Peel, V. Pettorino, J.-L. Starck, Z. Li, and J. Liu, Constraining neutrino masses with weak-lensing starlet peak counts, Phys. Rev. D **102**, 103531 (2020).
[50] C. Hahn, F. Villaescusa-Navarro, E. Castorina, and R. Scoccimarro, Constraining m_ν with the bispectrum. Part I. Breaking parameter degeneracies, J. Cosmol. Astropart. Phys. 03 (2020) 040.
[51] C. Hahn and F. Villaescusa-Navarro, Constraining m_ν with the bispectrum II: The total information content of the galaxy bispectrum, J. Cosmol. Astropart. Phys. 04 (2021) 029.
[52] C. Uhlemann, O. Friedrich, F. Villaescusa-Navarro, A. Banerjee, and S. Codis, Fisher for complements: Extracting cosmology and neutrino mass from the counts-in-cells PDF, Mon. Not. R. Astron. Soc. **495**, 4006 (2020).
[53] E. Massara, F. Villaescusa-Navarro, S. Ho, N. Dalal, and D. N. Spergel, Using the Marked Power Spectrum to Detect the Signature of Neutrinos in Large-Scale Structure, Phys. Rev. Lett. **126**, 011301 (2021).
[54] A. E. Bayer, F. Villaescusa-Navarro, E. Massara, J. Liu, D. N. Spergel, L. Verde, B. D. Wandelt, M. Viel, and S. Ho, Detecting neutrino mass by combining matter clustering, halos, and voids, Astrophys. J. **919**, 24 (2021).
[55] C. D. Kreisch, A. Pisani, F. Villaescusa-Navarro, D. N. Spergel, B. D. Wandelt, N. Hamaus, and A. E. Bayer, The GIGANTES dataset: Precision cosmology from voids in the machine learning era, arXiv:2107.02304.
[56] M. Cataneo, L. Lombriser, C. Heymans, A. J. Mead, A. Barreira, S. Bose, and B. Li, On the road to percent accuracy: Non-linear reaction of the matter power spectrum to dark energy and modified gravity, Mon. Not. R. Astron. Soc. **488**, 2121 (2019).
[57] M. Cataneo, J. D. Emberson, D. Inman, J. Harnois-Draps, and C. Heymans, On the road to percent accuracy III. Non-linear reaction of the matter power spectrum to massive neutrinos, Mon. Not. R. Astron. Soc. **491**, 3101 (2020).
[58] C. Pedersen, A. Font-Ribera, T. D. Kitching, P. McDonald, S. Bird, A. Slosar, K. K. Rogers, and A. Pontzen, Massive neutrinos and degeneracies in lyman-alpha forest simulations, J. Cosmol. Astropart. Phys. 04 (2020) 025.
[59] J. Maldacena, Non-Gaussian features of primordial fluctuations in single field inflationary models, J. High Energy Phys. 05 (2003) 013.
[60] P. Creminelli, A. Nicolis, L. Senatore, M. Tegmark, and M. Zaldarriaga, Limits on non-Gaussianities from WMAP data, J. Cosmol. Astropart. Phys. 05 (2006) 004.
[61] E. Komatsu, J. Dunkley, M. R. Nolta, C. L. Bennett, B. Gold, G. Hinshaw, N. Jarosik, D. Larson, M. Limon, L. Page *et al.*, Five-year Wilkinson microwave anisotropy probe observations: Cosmological interpretation, Astrophys. J. Suppl. Ser. **180**, 330 (2009).
[62] U. Seljak, Extracting Primordial Non-Gaussianity without Cosmic Variance, Phys. Rev. Lett. **102**, 021302 (2009).
[63] Y. Akrami *et al.* (Planck Collaboration), Planck 2018 results. IX. Constraints on primordial non-Gaussianity, Astron. Astrophys. **641**, A9 (2020).
[64] X. Chen, Primordial non-Gaussianities from inflation models, Adv. Astron. **2010**, 1 (2010).

[65] P. D. Meerburg *et al.*, Primordial non-Gaussianity, arXiv:1903.04409.
[66] M. Zennaro, J. Bel, F. Villaescusa-Navarro, C. Carbone, E. Sefusatti, and L. Guzzo, Initial conditions for accurate N-body simulations of massive neutrino cosmologies, Mon. Not. R. Astron. Soc. **466**, 3244 (2017).
[67] V. Springel, The cosmological simulation code GADGET-2, Mon. Not. R. Astron. Soc. **364**, 1105 (2005).
[68] A. Font-Ribera, P. McDonald, N. Mostek, B. A. Reid, H.-J. Seo, and A. Slosar, DESI and other dark energy experiments in the era of neutrino mass measurements, J. Cosmol. Astropart. Phys. 05 (2014) 023.
[69] F. Villaescusa-Navarro *et al.*, The Quijote simulations, Astrophys. J. **250**, 2 (2020).
[70] A. Lewis, A. Challinor, and A. Lasenby, Efficient computation of cosmic microwave background anisotropies in closed Friedmann-Robertson-Walker models, Astrophys. J. **538**, 473 (2000).
[71] U. Seljak, G. Aslanyan, Y. Feng, and C. Modi, Towards optimal extraction of cosmological information from nonlinear data, J. Cosmol. Astropart. Phys. 12 (2017) 009.
[72] F. Simpson and S. Bridle, Illuminating dark energy with cosmic shear, Phys. Rev. D **71**, 083501 (2005).
[73] J. M. Zorrilla Matilla, Z. Haiman, A. Petri, and T. Namikawa, Geometry and growth contributions to cosmic shear observables, Phys. Rev. D **96**, 023513 (2017).
[74] J. Kuruvilla and N. Aghanim, Information content in mean pairwise velocity and mean relative velocity between pairs in a triplet, Astron. Astrophys. **653**, A130 (2021).
[75] C. D. Kreisch, F.-Y. Cyr-Racine, and O. Doré, Neutrino puzzle: Anomalies, interactions, and cosmological tensions, Phys. Rev. D **101**, 123505 (2020).
[76] S. Cheng and B. Ménard, Weak lensing scattering transform: Dark energy and neutrino mass sensitivity, Mon. Not. R. Astron. Soc. **507**, 1012 (2021).
[77] G. Valogiannis and C. Dvorkin, Towards an optimal estimation of cosmological parameters with the wavelet scattering transform, arXiv:2108.07821.
[78] A. Blanchard, S. Camera, C. Carbone, V. F. Cardone, S. Casas, S. Clesse, S. Ili, M. Kilbinger, T. Kitching *et al.*, Euclid preparation, Astron. Astrophys. **642**, A191 (2020).
[79] S. Yahia-Cherif, A. Blanchard, S. Camera, S. Casas, S. Ili, K. Markovi, A. Pourtsidou, Z. Sakr, D. Sapone, and I. Tutusaus, Validating the fisher approach for stage iv spectroscopic surveys, Astron. Astrophys. **649**, A52 (2021).
[80] N. Bhandari, C. D. Leonard, M. M. Rau, and R. Mandelbaum, Fisher matrix stability, arXiv:2101.00298.